

# Electrochemical sensitive detection of 2, 6-dimethylphenol in petrochemical wastewater based on ferroporphyrin modified glassy carbon electrode

Quan Li<sup>1,\*</sup>, Dianhui Wang<sup>2</sup>

<sup>1</sup> College of Materials Sciences and Engineering, Henan Institute of Technology, Xinxiang 453000, Henan, China

<sup>2</sup> AnYang Research Institute of Ecologic and Environmental science, Anyang 455000, Henan, China

\*E-mail: [johnli258@163.com](mailto:johnli258@163.com)

Received: 23 March 2022 / Accepted: 28 April 2022 / Published: 6 June 2022

Detection of 2, 6-dimethylphenol in petroleum wastewater is essential in the environmental field. A glassy carbon electrode (GCE) modified with ferroporphyrin (FP) was prepared in this work. XRD and FTIR were used to characterize the interface of FP. FP can increase the active site and effective catalytic area of the electrode. Compared with bare glass carbon electrode GCE, FP/GCE has a more apparent electrochemical response, stronger current background value, and higher sensitivity, which can meet the detection of 2, 6-dimethylphenol. The concentration, enrichment time, enrichment potential, electrolyte type, and pH of FP were optimized. Under optimal conditions, the proposed sensor can detect 2, 6-dimethylphenol linearly in the concentration range of 8  $\mu\text{M}$ ~0.1 mM. The detection limit can be calculated to be 1  $\mu\text{M}$ . The preparation process of a modified electrode is convenient and straightforward, with good stability and repeatability. It has an apparent electrochemical response, high detection sensitivity, and low detection limit, providing a new method and idea for detecting 2, 6-dimethylphenol in petroleum wastewater.

**Keywords:** Electrochemical sensor; 2, 6-dimethylphenol; Petrochemical wastewater; Ferriporphyrin; Environmental analysis

## 1. INTRODUCTION

Crude oil is a thick, dark brown liquid extracted directly from the ground, a natural hydrocarbon. Crude oil is processed and refined to form petroleum products such as liquefied petroleum gas, gasoline, kerosene, diesel oil, lubricating oil, and asphalt [1–3]. According to the types and compositions of hydrocarbon, crude oils can be divided into paraffin-rich, cyclo-rich, etc. The boiling points of different components in petroleum are different, and different boiling points can be obtained by heating distillation of petroleum with this characteristic [4–6]. Due to the variety of products produced by refineries and

related chemical plants, the nature of raw materials, processing processes, and technological methods are different, and the pollutant components in wastewater are very complex [7–9].

Naphtha aromatization modification technology converts naphtha or dilutes hydrocarbons from light hydrocarbons such as oilfield condensate, straight-line naphtha, coking gasoline, and reforming residual oil to aromatic hydrocarbons using a proprietary series of catalysts [10–13]. The introduction of this technique increases the probability of phenol production. Heavy oil contains many reconstituted components, which cannot be completely vaporized at the nozzle exit, so there is a certain proportion of un-vaporized components [14–18]. The vaporized portion is subjected to conventional catalytic cracking, and the un-vaporized portion is subjected to conventional catalytic cracking if it absorbs surrounding heat in the mixing zone and vaporizes. The part that cannot be vaporized will go into the hole of the catalyst for thermal cracking or intermediate products of catalytic cracking. A large amount of acid-containing wastewater is produced during the catalytic cracking process of heavy oil, and the concentration of volatile phenol in the wastewater discharged during the separation of oil and water in the catalytic cracking fractionator is very high [19,20].

Phenolic compounds are highly toxic organic pollutants [21]. Some phenols, such as polychlorophenols, are highly toxic and difficult to degrade. Phenolic wastewater is one of the most harmful and widely polluted industrial wastewater globally. Phenolic wastewater discharged into the water body by industrial wastewater will affect and harm water quality, vegetation, and aquatic organisms to a certain extent [22–24]. Any discharge of phenol-containing wastewater can penetrate farmland through water flow and water bodies and affect the growth of crops. If people drink water from contaminated waters or eat aquatic products and crops from contaminated areas, their health will be directly affected [25,26]. Therefore, it is very important to detect phenols in petroleum wastewater. At present, the primary methods for determining phenols are liquid chromatography, gas chromatography, high-performance liquid chromatography, and the combination of these methods [27,28]. However, these methods require expensive instruments, complex operations, troublesome pre-processing, and higher operator requirements. Electrochemical analysis has the advantages of high sensitivity, simple operation, good selectivity, and low cost, so it can be used to detect the content of phenolic pollutants in the water environment [29–31]. In this work, we report an iron porphyrin modified electrode to detect 2, 6-dimethylphenol. Porphyrin compounds because of their intense aroma, easy adsorption, and strong structure [32,33]. Their metal coordination compounds are widely used in medicine, bionics, catalysis, and chemistry. In this study, iron porphyrin was used as the modification material of the electrode, which could increase the specific surface area of the electrode and catalyze the oxidation current of 2, 6-dimethylphenol. Thus, the electrochemical sensor constructed could be used to detect 2, 6-dimethylphenol content in petroleum wastewater.

## 2. EXPERIMENTAL

### 2.1. Synthesis of iron porphyrin (FP)

400 mg of 5, 10, 15, 20-tetraphenylporphyrin-Fe and 1.6 g of  $\text{AlCl}_3$  were added to a 100 mL round-bottled flask. 40 mL  $\text{CHCl}_3$  was added to a dry three-neck flask, protected with nitrogen for

reaction at 60 °C for 48 h, and cooled to indoor temperature. After centrifugation, they were washed with anhydrous ethanol, 3 M HCl solution, and methanol 3 times. The product was dried in a vacuum at 120 °C, and the black powder was FP.

## 2.2. Preparation of FP modified electrode

Firstly, a glassy carbon electrode (GCE, 3 mm) was prepared and polished clean on 3000 mesh sandpaper. Then, the electrodes were polished to mirror the surface with Al<sub>2</sub>O<sub>3</sub> alumina polishing powder of 1.5 μm, 0.5 μm, and 50 nm, respectively. Then, GCE was washed by ultrasonic for 3 min in dilute nitric acid solution, ethanol, and ultra-pure water, respectively, and waited for natural air drying. The FP was added to water by ultrasonic until it was completely dispersed in an aqueous solution. Then 0.5 mg/mL FP dispersion was mixed with 0.5% chitosan, and then 5 μL was dropped on the surface of the polished and dried electrode with a pipette. Cyclic voltammetry (CV) has been used for 2, 6-dimethylphenol sensing. The scan window was between 0.3 to 1.0 V and the scan rate was 50 mV/s. A differential pulse voltammetry (DPV) signal between 0.4 and 0.9 V was collected (pulse amplitude: 50 mV; pulse width: 0.05 s; pulse period: 0.5 s). A disodium phosphate-citric acid buffer solution has been used as electrolyte.

## 3. RESULTS AND DISCUSSION

The synthesized FP was characterized by XRD. The test scanning speed was 1°/min, and the scanning range was 5-40°. The scanning results are shown in Figure 1A. There is no prominent diffraction peak in the XRD pattern, and the XRD curve is consistent with the literature, indicating that the material has an amorphous structure [34].

Subsequently, the synthesized product was characterized by infrared spectroscopy. Under the irradiation of an infrared lamp, 1 mg of synthesized FP and 100 mg of pure KBr were mixed and ground evenly. The mixture was pressed into a transparent sample with an infrared tablet grinding tool, and the infrared spectrum was determined by an FT-IR absorption spectrometer. As shown in Figure 1B, due to the coupling effect, there is a C-H absorption peak at 1650~1400 cm<sup>-1</sup> and a C-C absorption peak at 800 ~ 700 cm<sup>-1</sup> [35,36]. The absorption rate moves to a low wavenumber and the peak intensity weakens. Due to the absorption peak at 750 cm<sup>-1</sup>, benzene ring coupling forms a network structure. The Fe-N characteristic vibration of metallic porphyrins was observed at about 1000 cm<sup>-1</sup>, and there were metal cations in the middle of the porphyrin ring [37], which proved that the polymer was successfully synthesized.

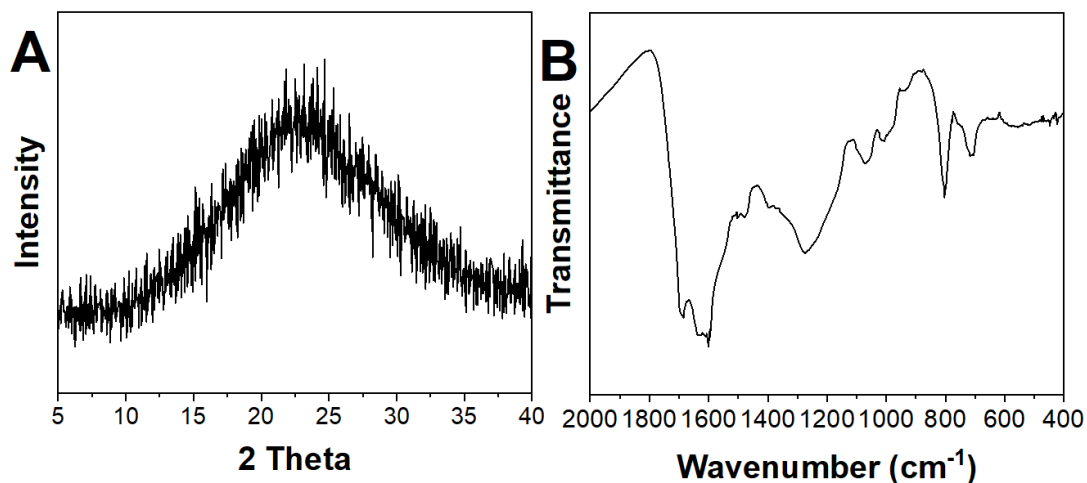


**Figure 1.** (A) XRD pattern and (B) FTIR spectrum of FP.

Cyclic voltammetry was performed in potassium ferricyanide (5.0 mM, containing 0.2 M KCl) solution using GCE and FP/GCE as working electrodes, platinum electrode as a counter electrode, and Ag/AgCl as a reference electrode, respectively. The results are shown in Figure 2. A reversible redox peak and current intensity of GCE in potassium ferricyanide solution were 0.2 V and 22.43  $\mu\text{A}$ , respectively.

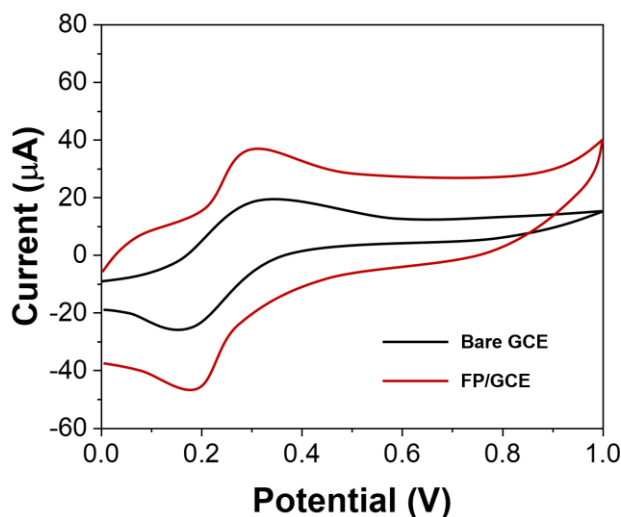


**Figure 2.** CV curves of GCE and FP/GCE in 5 mM  $[\text{Fe}(\text{CN})_6]^{3-/4-}$  + 0.2 M KCl.

A pair of reversible redox peaks of FP/GCE also appeared in potassium ferricyanide solution with a potential difference of 0.1 V and a current intensity of 38.28  $\mu\text{A}$ . Because  $\text{K}_3[\text{Fe}(\text{CN})_6]$  and  $\text{K}_4[\text{Fe}(\text{CN})_6]$  are reversible redox electric pairs, the effective area of electroactivity of the electrode can be calculated by its electrochemical response characteristics [38]. According to the Randles-Sevcik formula, the electroactive area of GCE and FP/GCE can be calculated as 0.204  $\text{cm}^2$  and 0.311  $\text{cm}^2$ , respectively. In conclusion, compared with bare GCE and FP modified electrodes, the electrochemical

signal increases, the current background is significantly enhanced, and the peak current value increases by 2 times. This indicates that the modified material increases the electrode's active site and effective catalytic area and plays an optimization role on the electrode [39]. At the same time, it also shows that FP has good electron conductivity and high catalytic activity.

GCE and FP/GCE were respectively used for cyclic voltammetry detection of 2, 6-dimethylphenol solution containing PBS (0.1 M, pH=7.0) at 50  $\mu$ M. The results are shown in Figure 3A. As can be seen from the figure, only an oxidation peak appeared in both of them, but no reduction peak appeared, indicating that the electrocatalytic reaction process of 2, 6-dimethylphenol on the electrode was irreversible [40]. At the same time, 6-dimethylphenol had little response on GCE, with a weak oxidation peak at +0.738 V and an obvious oxidation peak at FP/GCE, and the peak potential shifted to +0.686 V. Compared with GCE, the oxidation peak current value of FP/GCE increases by more than 3 times. This may be because the modified material increases the conductivity of the electrode, effectively promoting the electron transfer of the electrode reaction. This showed that FP/GCE had an excellent electrical activity and a good response to 2, 6-dimethylphenol.

We also studied the differential pulse voltammetry (DPV) detection of 2, 6-dimethylphenol with 50  $\mu$ M of FP/GCE under the same conditions, and the results are shown in Figure 3B. It is shown that there is an oxidation peak, FP/GCE in the + 0.67v, and there is an oxidation peak in the + 0.628 v, and the peak potential is negative. Moreover, the oxidation peak current value of the modified electrode increased 5.2 times than that of the bare glassy carbon electrode, indicating that the modified electrode had excellent catalytic oxidation of 2, 6-dimethylphenol [41]. Since the peak shape of DPV was sharper and more evident than that of cyclic voltammetry, differential pulse voltammetry was used to detect 2, 6-dimethylphenol.

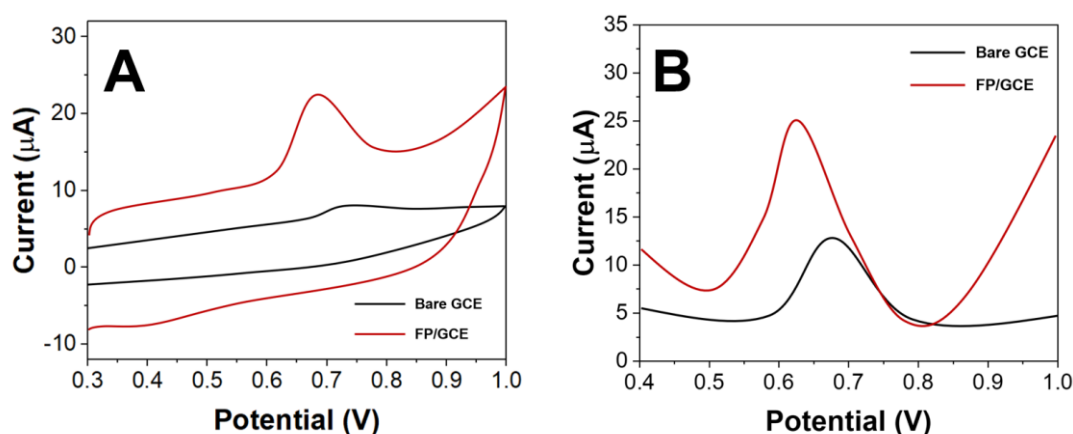


**Figure 3.** (A) CVs and (B) DPVs of GCE and FP/GCE towards 50  $\mu$ M 2, 6-dimethylphenol in disodium phosphate-citric acid buffer solution.

The DPV was used to study the relationship between the concentration of FP dispersive solution (0.1-0.9 mg/mL) and the peak current value of 2, 6-dimethylphenol oxidation of 50  $\mu$ M. The results are shown in Figure 4A. With the gradual increase of FP concentration, the corresponding oxidation peak current value increases first and then decreases, and the peak potential shifts slightly positively [42]. The

current reaches its maximum at 0.5 mg/mL. This is because, as the concentration of FP increases, the electron transfer rate increases. However, when the concentration is too large, the stability will deteriorate, resulting in peak potential deviation, oxidation peak current value decreases. Therefore, 0.5 mg/mL was selected as the optimal concentration in the following experiments.

The value of oxidation peak current is closely related to the content of detected substances on the electrode surface, and the enrichment potential is one of the main factors affecting the enrichment effect [43]. Therefore, the time-current method was used to study the influence of different enrichment potentials on the oxidation peak current value of 2, 6-dimethylphenol at a concentration of 50  $\mu\text{M}$  in the range of  $-0.1\text{V} \sim +0.4\text{V}$ . The results are shown in Figure 4B. As can be seen from the figure, the oxidation peak current value of 2, 6-dimethylphenol increased first and then decreased with enrichment potential. When the enrichment potential is + 0.2 V, the oxidation peak current value is the largest and the peak shape is sharper, so + 0.2 V is the best enrichment potential.

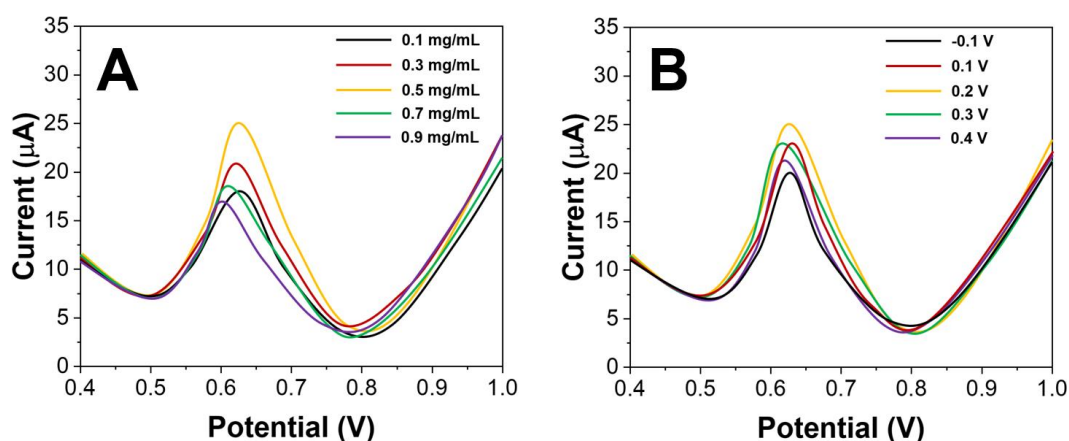


**Figure 4.** Effect of (A) concentration FP dispersion and (B) accumulation potential in the sensing performance.

In trace analysis, appropriate enrichment time can effectively improve the sensitivity. If the enrichment time is too short, the sensitivity will be too low, while if the enrichment time is too long, the background value will become more significant, and measurement time will be prolonged, which does not achieve the purpose of fast and straightforward. Therefore, the influence of different enrichment times on oxidation peak current value of 50  $\mu\text{M}$  2, 6-dimethylphenol was studied by controlling other conditions unchanged [44]. The results are shown in Figure 5A. As can be seen from the figure, the oxidation peak current value increases with the increase of enrichment time. When the enrichment time exceeds 150 s, the oxidation peak current increases slowly and tends to be stable. This indicates that adsorption equilibrium is reached, so 300 s is chosen as the best enrichment time.

We used DPV to compare the concentration of 50  $\mu\text{M}$  2, 6 - dimethylphenol in the different supporting electrolyte solutions ( $\text{NaH}_2\text{PO}_4$ -CA buffer solution,  $\text{Na}_2\text{HPO}_4$ - $\text{KH}_2\text{PO}_4$  buffer solution, CA- $\text{NaCA}$  buffer solution,  $\text{NaCl}$ ,  $\text{NH}_4\text{Cl}$ - $\text{NH}_3(\text{aq})$  buffer solution, CA- $\text{CH}_3\text{COONa}$  buffer solution) of the

electrochemical behavior, the result is shown in Figure 5B. As can be seen from the figure, when  $\text{NH}_4\text{Cl-NH}_3(\text{aq})$  buffer solution and  $\text{NaCl}$  buffer solution are used as supporting electrolytes, the oxidation peak shape is passivated, and the electrochemical response signal is poor [45]. However, when  $\text{NaH}_2\text{PO}_4\text{-CA}$  buffer solution,  $\text{Na}_2\text{HPO}_4\text{-KH}_2\text{PO}_4$  buffer solution,  $\text{CA-NaCA}$  buffer solution,  $\text{CA-NaCA}$  buffer solution, and  $\text{CA-CH}_3\text{COONa}$  buffer solution as supporting electrolytes, the peak shape of chlorophenol, electrochemical response signal is obvious, higher sensitivity [46]. In comparison, the current background response and oxidation peak current value of disodium hydrogen  $\text{NaH}_2\text{PO}_4\text{-CA}$  buffer solution as supporting electrolyte are better than the other five buffer solutions. Therefore,  $\text{NaH}_2\text{PO}_4\text{-CA}$  buffer solution was selected as the best supporting electrolyte.

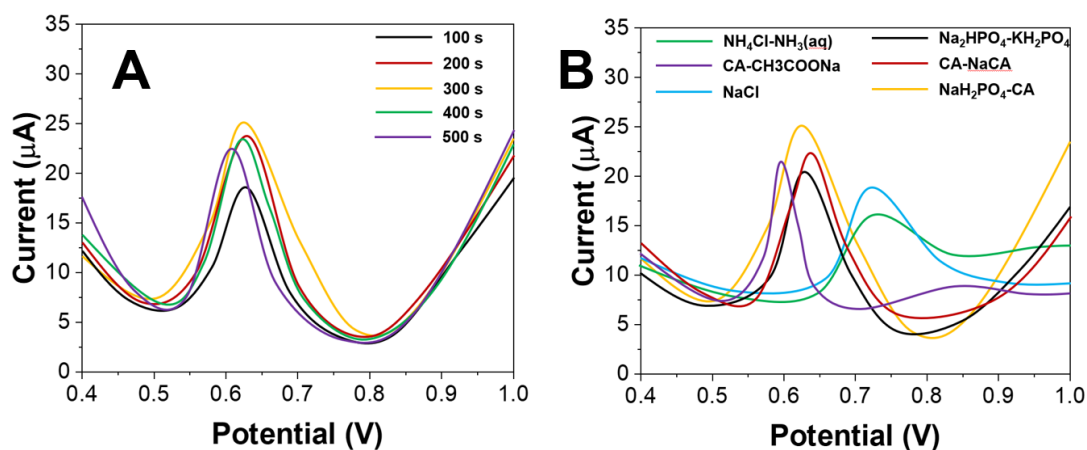


**Figure 5.** Effect of (A) accumulation time and (B) electrolyte type in the sensing performance.

The results show that the pH of the supporting electrolyte affects the oxidation peak current of 2, 6-dimethylphenol. Therefore, DPV was used to study the electrochemical behavior of 50  $\mu\text{M}$  2, 6-dimethylphenol at pH 4.0~8.0 with 0.1 M  $\text{NaH}_2\text{PO}_4\text{-CA}$  buffer solution. The results are shown in Figure 6A. As can be seen from the figure, within a specific pH range, the oxidation peak current value of 2, 6-dimethylphenol also increases with the increase of pH. This indicates that increasing pH can improve the sensitivity of the modified electrode to 2, 6-dimethylphenol detection. When pH=6.0, the oxidation peak current value reaches the maximum and the peak shape is the best. When the oxidation peak current exceeds 6.0, it tends to decrease. At the same time, with the increase of pH, the oxidation peak potential moves to the negative direction [47]. This may be because the oxidation reaction process involves protons. When the pH is too high, the number of protons in the solution is insufficient, which affects the electrode reaction and leads to the reduction of the oxidation peak current value.

The oxidation peak potential has an obvious linear relationship with pH within the range of pH, as shown in Figure 6B. According to the figure, the linear equation is  $E_p = -0.0571\text{pH} + 1.012$ , and the correlation coefficient is  $R = 0.9984$ . The slope was  $-57.1 \text{ mV/pH}$ , close to the theoretical value  $-59.2 \text{ mV/pH}$ , indicating that the same number of electrons and protons were involved in the electrocatalytic

oxidation of 2, 6-dimethylphenol on FP/GCE electrode. Figure 7 shows the possible oxidation mechanism of 2, 6-dimethylphenol.

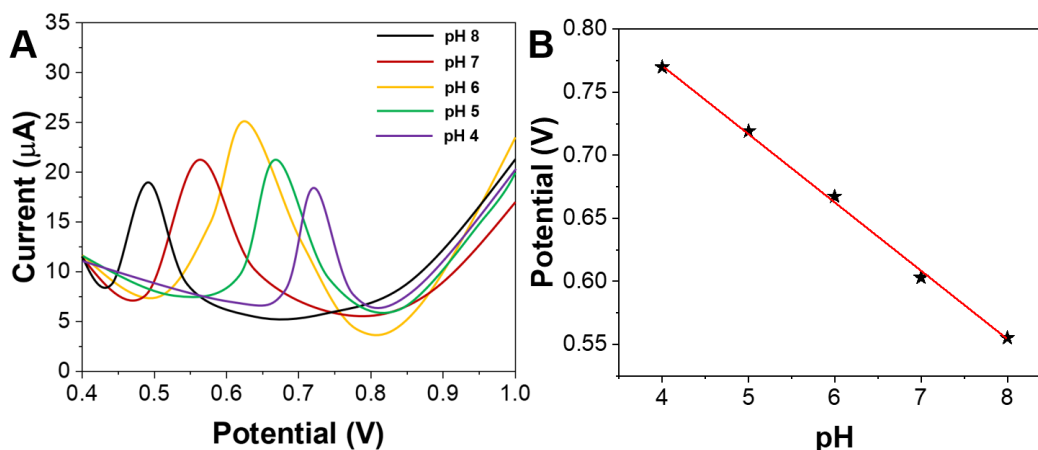


**Figure 6.** (A) Effect of pH on the sensing performance. (B) Relationship between oxidation peak potential and pH.

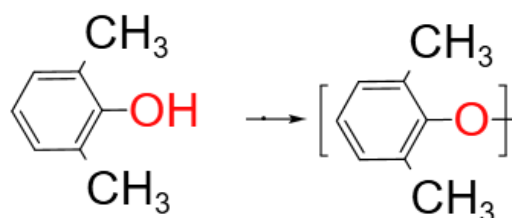


**Figure 7.** Possible oxidation mechanism of 2, 6-dimethylphenol

Under optimized conditions, FP/GCE was used to detect 2, 6-dimethylphenol at a series of concentrations within the voltage range of +0.4~+0.9 V by differential pulse voltammetry. The results are shown in Figure 8A. As seen from the figure, the oxidation peak current value and oxidation peak area of chlorophenol in NaH<sub>2</sub>PO<sub>4</sub>-CA buffer solution increased with the increase of concentration. This indicates that the modified electrode has a good response and high sensitivity to 2, 6-dimethylphenol. With 2, 6-dimethylphenol concentration as the abscissa and oxidation peak current value as the ordinate, the IP-C relationship curve was made, and the results were shown in Figure 8B. The results showed that the concentration of 2, 6-dimethylphenol showed a linear relationship with the oxidation peak current value in the range of 5 µM~0.1 mM. The detection limit can be calculated to be 1 µM. Table 1 shows the analytical performance comparison with previous literature. It can be seen that the proposed FP/GCE exhibited an excellent sensing performance compared with previous reports.

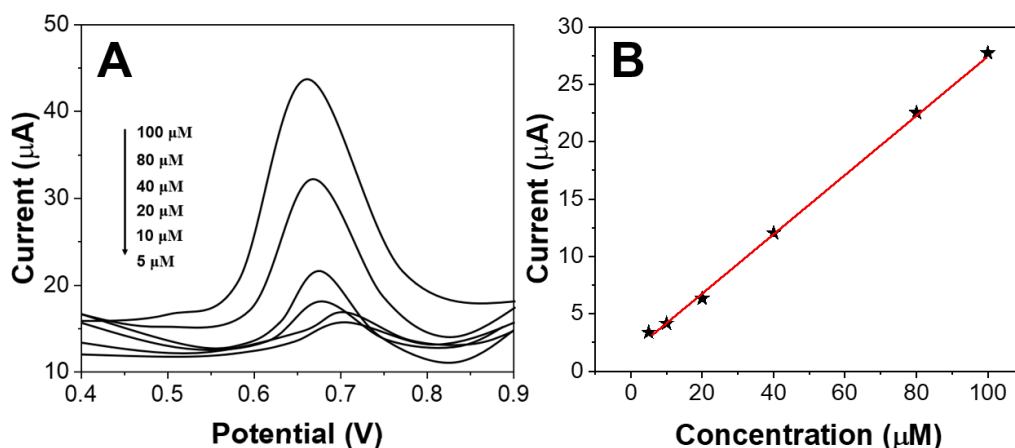


**Figure 8.** (A) Differential pulse voltammogram of FP/GCE towards different concentrations of 2, 6-dimethylphenol. (B) Correlation between concentration and peak current value.

**Table 1.** Comparison of previously reported 2, 6-dimethylphenol detection with this work.

Method	LR	LOD	Ref
Capillary electrochromatography	0.0032 to 0.014 mg/kg	2.72 mg/kg	[48]
Spectrophotometry	50 µM~200 mM	-	[49]
Spectrofluorometry	0.002 µg/mL to 0.1 µg/mL	0.0008 µg/mL	[50]
Electrochemistry	5 µM~0.1 mM	1 µM	This work

We tested the stability of the electrode. The same FP/GCE was used to determine the concentration of 2, 6-dimethylphenol at 30 µM for 7 times in parallel. The results show that the relative standard deviation of oxidation peak current value is 2.34% after 7 times of parallel measurement. Then the modified electrode was placed in the refrigerator at 4°C for 7 days, and DPV was used to detect 2, 6-dimethylphenol at the same concentration again. The results show that the oxidation peak current decreases by 8.43% and the peak potential remains unchanged. In conclusion, the prepared FP/GCE electrode has good stability.

At the same time, six GCE were modified, and the prepared FP/GCE was used for parallel detection of the above-mentioned concentration of detection solution. The relative standard deviation of the oxidation peak current of 2, 6-dimethylphenol was 2.87%. The test results show that the prepared FP/GCE electrode has good reproducibility.

In order to investigate the electrochemical detection effect of FP/GCE on 2, 6-dimethylphenol in actual petroleum wastewater, artificial petroleum wastewater was prepared as a practical sample. The results are shown in Table 2, indicating that the proposed electrochemical analysis method has a good recovery rate.

**Table 2.** Test results of artificial petrochemical wastewater samples and their recovery rates (n=5).

Sample No.	Found ( $\mu\text{M}$ )	Added ( $\mu\text{M}$ )	Found ( $\mu\text{M}$ )	Recovery (%)	RSD (%)
1	-	10.00	10.41	104.10	3.10
2	-	20.00	19.22	96.10	2.12
3	-	40.00	42.19	105.48	2.42

#### 4. CONCLUSION

In this work, a chemically synthesized FP was proposed for surface modification of the GCE electrode. The electrochemical behavior of 2, 6-dimethylphenol on the modified electrode was investigated by CV and DPV. The experimental results show that FP increases the electrode's active site and effective catalytic area. Compared with bare glass carbon electrode GCE, FP/GCE has a more apparent electrochemical response, stronger current background value, and higher sensitivity, which can meet the detection of 2, 6-dimethylphenol. We also optimized the detection parameters. The preparation process of the modified electrode is simple and convenient and has good stability and repeatability. It has an apparent electrochemical response, high detection sensitivity, and low detection limit, providing a new method and idea for detecting 2, 6-dimethylphenol in petroleum wastewater.

#### References

1. A. Arvin, M. Hosseini, M.M. Amin, G.N. Darzi, Y. Ghasemi, *Biochem. Eng. J.*, 144 (2019) 157.
2. J.F. de Melo, D.M. de Araújo, D.R. da Silva, C.A.M. Huitle, P. Villegas-Guzman, *Int J Electrochem Sci*, 15 (2020) 10262.
3. D. Clematis, M. Panizza, *Curr. Opin. Electrochem.*, 30 (2021) 100844.
4. D. Clematis, M. Panizza, *Curr. Opin. Electrochem.*, 30 (2021) 100844.
5. H. Karimi-Maleh, Y. Orooji, F. Karimi, M. Alizadeh, M. Baghayeri, J. Rouhi, S. Tajik, H. Beitollahi, S. Agarwal, V.K. Gupta, *Biosens. Bioelectron.* (2021) 113252.
6. H. Karimi-Maleh, A. Khataee, F. Karimi, M. Baghayeri, L. Fu, J. Rouhi, C. Karaman, O. Karaman, R. Boukherroub, *Chemosphere* (2021) 132928.
7. M. Rayung, M.M. Aung, S.C. Azhar, L.C. Abdullah, M.S. Su'ait, A. Ahmad, S.N.A.M. Jamil, *Materials*, 13 (2020) 838.
8. S. Sarmin, B. Ethiraj, M.A. Islam, A. Ideris, C.S. Yee, Md.M.R. Khan, *Sci. Total Environ.*, 695 (2019) 133820.
9. H. Karimi-Maleh, F. Karimi, L. Fu, A.L. Sanati, M. Alizadeh, C. Karaman, Y. Orooji, *J. Hazard. Mater.*, 423 (2022) 127058.
10. A. Medel, F. Lugo, Y. Meas, C.A. Martínez-Huitle, M.A. Rodrigo, O. Scialdone (Eds.), *Electrochem. Water Wastewater Treat.*, Butterworth-Heinemann, (2018), pp. 365.
11. H. Li, X. Kuang, X. Shen, J. Zhu, *Environ. Technol.*, 43 (2022) 431.
12. Y. Zheng, D. Wang, X. Li, Z. Wang, Q. Zhou, L. Fu, Y. Yin, D. Creech, *Biosensors*, 11 (2021) 403.

13. H. Karimi-Maleh, M. Alizadeh, Y. Orooji, F. Karimi, M. Baghayeri, J. Rouhi, S. Tajik, H. Beitollahi, S. Agarwal, V.K. Gupta, S. Rajendran, S. Rostamnia, L. Fu, F. Saberi-Movahed, S. Malekmohammadi, *Ind. Eng. Chem. Res.*, 60 (2021) 816.
14. V.K. Sandhwar, D. Saxena, S. Verma, K.K. Garg, B. Prasad, *Sep. Sci. Technol.*, 56 (2021) 2300–2309.
15. Y. He, D. Zhao, H. Lin, H. Huang, H. Li, Z. Guo, *Curr. Opin. Electrochem.* (2021) 100878.
16. D. Wang, D. Li, L. Fu, Y. Zheng, Y. Gu, F. Chen, S. Zhao, *Sensors*, 21 (2021) 8216.
17. Y. Wang, L. Chen, T. Xuan, J. Wang, X. Wang, *Front. Chem.*, 9 (2021) 569.
18. H. Karimi-Maleh, C. Karaman, O. Karaman, F. Karimi, Y. Vasseghian, L. Fu, M. Baghayeri, J. Rouhi, P. Senthil Kumar, P.-L. Show, S. Rajendran, A.L. Sanati, A. Mirabi, *J. Nanostructure Chem.* (2022) in-press.
19. J. Xu, X. Xiao, Z. Zhang, Y. Wu, D.T. Boyle, H.K. Lee, W. Huang, Y. Li, H. Wang, J. Li, *Nano Lett.*, 20 (2020) 8719.
20. A. Arvin, M. Hosseini, M.M. Amin, G. Najafpour Darzi, Y. Ghasemi, *J. Environ. Health Sci. Eng.*, 17 (2019) 305.
21. J. Lu, M. Cheng, C. Zhao, B. Li, H. Peng, Y. Zhang, Q. Shao, M. Hassan, *Ind. Crops Prod.*, 176 (2022) 114267.
22. E.J. Biddinger, M.A. Modestino, *Electrochem. Soc. Interface*, 29 (2020) 43.
23. A. Dargahi, M. Vosoughi, S.A. Mokhtari, Y. Vaziri, M. Alighadri, *Arab. J. Chem.*, 15 (2022) 103648.
24. L. Fu, A. Yu, G. Lai, *Chemosensors*, 9 (2021) 282.
25. A. Urriaga, *Curr. Opin. Electrochem.*, 27 (2021) 100691.
26. J. de J. Treviño-Reséndez, A. Medel, Y. Meas, *Curr. Opin. Electrochem.*, 27 (2021) 100690.
27. E. Ntagia, E. Fiset, L. Truong Cong Hong, E. Vaiopoulou, K. Rabaey, *J. Hazard. Mater.*, 388 (2020) 121770.
28. V. de Oliveira Campos, L.B. do Amaral, A.M.S. Solano, D.M. de Araújo, C.A. Martínez-Huitle, D.R. da Silva, *Int. J. Electrochem. Sci.*, 13 (2018) 7894.
29. S. Wohlmuth da Silva, C.D. Venzke, J. Bitencourt Welter, D.E. Schneider, J. Zoppas Ferreira, M.A. Siqueira Rodrigues, A. Moura Bernardes, *Int. J. Environ. Res. Public. Health*, 16 (2019) 816.
30. M. Dehboudeh, P. Dehghan, A. Azari, M. Abbasi, *J. Environ. Chem. Eng.*, 8 (2020) 104537.
31. J. Liang, W. Mai, J. Tang, Y. Wei, *Chem. Eng. J.*, 360 (2019) 15.
32. N. Yousefi, S. Pourfadakari, S. Esmaeili, A.A. Babaei, *Microchem. J.*, 147 (2019) 1075.
33. R. Raj, A. Tripathi, S. Das, M. Ghangrekar, *Case Stud. Chem. Environ. Eng.*, 4 (2021) 100129.
34. H. Zhou, Z. Li, S. Xu, L. Lu, M. Xu, K. Ji, R. Ge, Y. Yan, L. Ma, X. Kong, *Angew. Chem. Int. Ed.*, 60 (2021) 8976.
35. G.H. de Kruijff, T. Goschler, N. Beiser, A. Stenglein, O.M. Türk, S.R. Waldvogel, *Green Chem.*, 21 (2019) 4815.
36. Z. Bo, T. Zhibo, *Int J Electrochem Sci*, 15 (2020) 6177.
37. C. Gong, X. Ren, J. Han, Y. Wu, Y. Gou, Z. Zhang, P. He, *Chemosphere*, 286 (2022) 131582.
38. M. Adimi, S. Mohammad Mohebizadeh, M.M. Poor, S. Ghavamnia, A. Marjani, *Iran. J. Sci. Technol. Trans. Sci.*, 43 (2019) 2799.
39. H. Karimi-Maleh, A. Ayati, R. Davoodi, B. Tanhaei, F. Karimi, S. Malekmohammadi, Y. Orooji, L. Fu, M. Sillanpää, *J. Clean. Prod.*, 291 (2021) 125880.
40. S. Wei, X. Chen, X. Zhang, L. Chen, *Front. Chem.*, 9 (2021) 697.
41. R. Duan, X. Fang, D. Wang, *Front. Chem.*, 9 (2021) 361.
42. J. Liu, T. Yang, J. Xu, Y. Sun, *Front. Chem.*, 9 (2021) 488.
43. J. Li, S. Zhang, L. Zhang, Y. Zhang, H. Zhang, C. Zhang, X. Xuan, M. Wang, J. Zhang, Y. Yuan, *Front. Chem.*, 9 (2021) 339.
44. X. Qin, W. Guo, H. Yu, J. Zhao, M. Pei, *Anal. Methods*, 7 (2015) 5419.
45. O. Bunkoed, P. Raksawong, R. Chaowana, P. Nurerk, *Talanta*, 218 (2020) 121168.

46. W. Xu, Y. Wang, S. Liu, J. Yu, H. Wang, J. Huang, *New J. Chem.*, 38 (2014) 4931.
47. X. Shi, Y. Zuo, X. Jia, X. Wu, N. Jing, B. Wen, X. Mi, *Int J Electrochem Sci*, 15 (2020) 9683.
48. Y.S. Fung, Y.H. Long, *J. Chromatogr. A*, 907 (2001) 301.
49. A. Hartley, R. Asai, *Anal. Chem.*, 35 (1963) 1207.
50. W. Ma, Z. Liu, R. Cai, *Anal. Sci.*, 15 (1999) 963.

© 2022 The Authors. Published by ESG ([www.electrochemsci.org](http://www.electrochemsci.org)). This article is an open access article distributed under the terms and conditions of the Creative Commons Attribution license (<http://creativecommons.org/licenses/by/4.0/>).